

PROMPT PHOTONS AND DVCS AT HERA

J.C. HART

*Rutherford Appleton Laboratory, Chilton, DIDCOT, Oxfordshire OX11 0QX, England
(on behalf of the ZEUS and H1 collaborations)*

A recent analysis of prompt-photon events in ZEUS has led to a new determination of the effective transverse parton momentum in the proton. The observation of deeply virtual Compton scattering by ZEUS and H1, including a first measurement of the DVCS cross section at HERA by H1, is also reported.

1 Introduction

The production of real photons in high energy ep collisions (prompt photons) is of interest because it allows the parton level interactions to be investigated while minimising the complication of parton hadronisation. Two recent studies of prompt-photon production at HERA are reported in this paper.

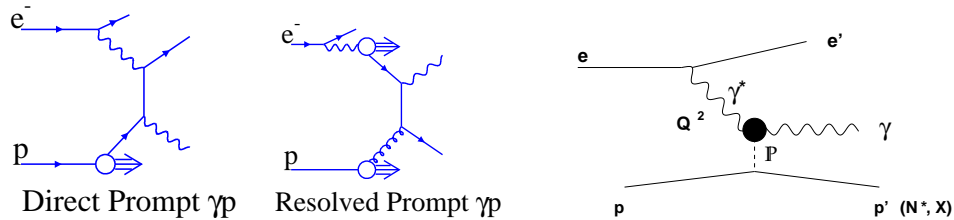


Figure 1: Typical diagrams for prompt photon production in direct and resolved photoproduction are shown on the left. The right-hand diagram is for DVCS.

The first reaction to be discussed is prompt-photon photoproduction where a real photon is produced directly from the hard interaction of a quasi-real photon. Both direct processes (where the entire photon participates in the interaction) and resolved processes (where the photon first fluctuates into a hadronic system) are possible as shown by the examples in Fig.1. ZEUS has used the direct process to determine $\langle k_T \rangle$, the effective transverse parton momentum in the proton.

The second process is deeply virtual Compton scattering (DVCS) in which a real photon is produced through the diffractive scattering of a virtual photon off the proton as shown in Fig.1 (right-hand diagram). DVCS makes it possible to study exclusive diffraction without the theoretical uncertainty introduced by the vector meson wave function. It is also sensitive to the skewed parton distributions which describe two-parton correlations in the proton. DVCS has been seen at HERA by both ZEUS and H1, and H1 has measured differential cross-sections.

2 Prompt photons in photoproduction and determination of $\langle k_T \rangle$

The ZEUS analysis of prompt photons is based on data taken at the HERA e-p collider in 1996-97 with positron and proton beam energies of 27.5 and 820 GeV, respectively. The ZEUS detector, including the uranium-scintillator calorimeter and central tracking detector (CTD), which are relevant for this study, have been described elsewhere.^{1,2,3}

The signature for prompt photon events was an isolated cluster of cells in the electromagnetic section of the ZEUS barrel calorimeter. At least one visible jet was required to determine $\langle k_T \rangle$. Events with the scattered positron seen in the calorimeter were rejected. This selected photoproduction events with $Q^2 \leq 1 \text{ GeV}^2$ where Q^2 is the virtuality of the incoming photon. The other event selection cuts were

$$\begin{aligned} E_T^\gamma &> 5 \text{ GeV} & -0.7 < \eta^\gamma < 0.9 \\ E_T^{jet} &> 5 \text{ GeV} & -1.5 < \eta^{jet} < 1.8 \end{aligned}$$

where η is the pseudorapidity, $\eta = -\ln \tan(\theta/2)$, and the polar angle θ is measured with respect to the proton beam. The photon isolation requirement was the absence of any other calorimeter cluster in a unit (η, ϕ) cone around the photon direction, where ϕ is the azimuthal angle.

Photons were distinguished from neutral mesons (π^0 and η^0) by virtue of their smaller cluster size in the calorimeter, as in previous ZEUS analyses.^{1,4} A cut of 3.25 cm was first applied to the cluster width in the z -direction (parallel to the proton beam) to enhance the photon purity. The fraction, f_{max} , of the total energy in a single calorimeter cell peaks near 1.0 for photons, but is flatter for π^0 and η^0 and is insensitive to the π^0/η^0 ratio. It was therefore used to make a statistical subtraction of the remaining π^0 and η^0 background.

The incoming photon energy for each event was estimated from $y_{JB} = \sum (E - p_z)/2E_e$, where the sum is over all energy flow objects⁵ with energy E and longitudinal momentum p_z and E_e is the incident positron beam energy. Limits of $0.2 < y_{JB} < 0.7$ were applied to remove beam-gas and deep inelastic scattering events. Direct photoproduction events were selected by applying a cut $x_\gamma^{\text{obs}} > 0.9$, where

$$x_\gamma^{\text{obs}} = \frac{1}{2E_e y_{JB}} \sum_{\gamma+jet} (E - p_z)$$

is the estimated fraction of the incoming photon energy in the QCD subprocess. Events passing this cut were nearly all from direct photoproduction.

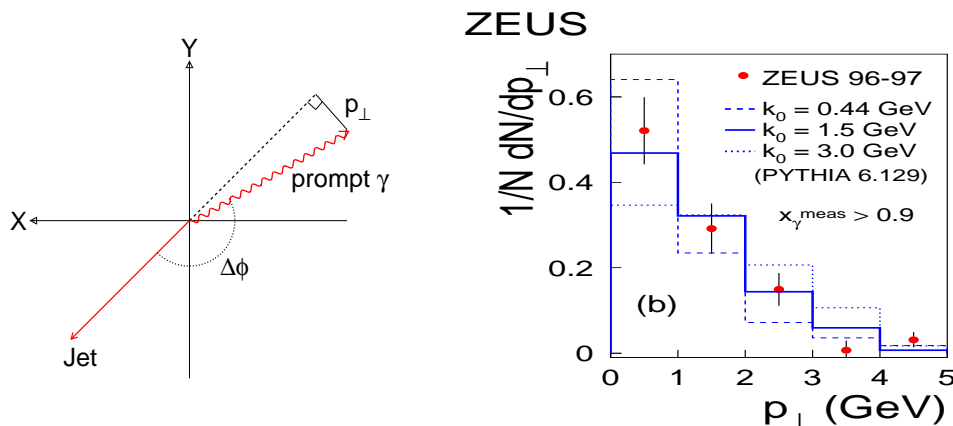


Figure 2: The left-hand diagram defines p_\perp . The X- and Y-axes are orthogonal to the proton beam. The distribution of p_\perp is shown on the right and compared to the predictions of PYTHIA for different values of k_0 .

To determine $\langle k_T \rangle$, the distribution of p_\perp , the momentum component of the photon perpendicular to the jet direction (see Fig. 2), was compared to the predictions of PYTHIA⁶ for

different values of the parameter k_0 , where $k_0 = \sqrt{4/\pi} \langle k_T^{\text{intr}} \rangle$ and $\langle k_T^{\text{intr}} \rangle$ is the mean absolute value of the intrinsic parton momentum in the proton in the PYTHIA model. The results may be seen in Fig.2 which shows that the data are compatible with a value of k_0 between about 0.4 GeV and 3.0 GeV. A fit to the p_\perp distribution was performed, with additional k_0 points, to find the optimal value of k_0 and hence $\langle k_T^{\text{intr}} \rangle$. The corresponding value of $\langle k_T \rangle$ was calculated by adding the parton shower contribution obtained from PYTHIA (~ 1.4 GeV) to give

$$\langle k_T \rangle = 1.69 \pm 0.18_{-0.20}^{+0.18} \text{ GeV.}$$

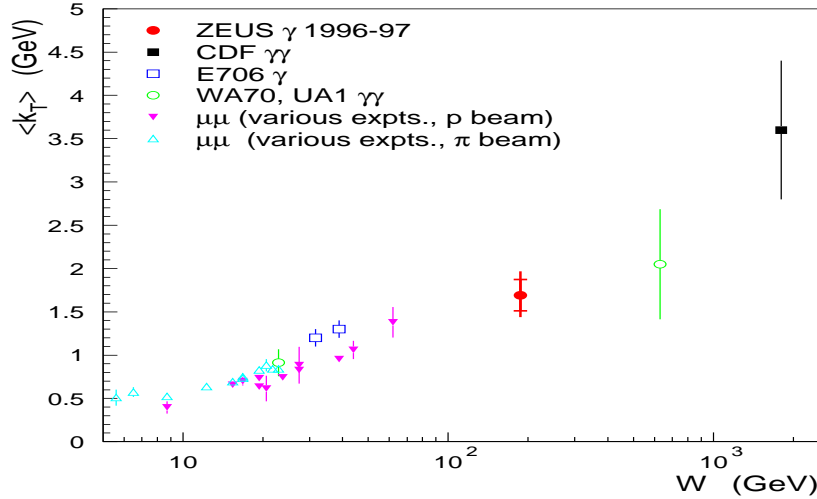


Figure 3: Measurements of $\langle k_T \rangle$ for a number of experiments, including the new ZEUS result, are plotted against the centre-of-mass energy for the colliding particles. For ZEUS, these are the photon and proton.

In Fig.3 this is plotted, together with mean $\langle k_T \rangle$ values from other experiments,^{7,8} as a function of the centre-of-mass energy, W , of the incoming particles. It can be seen that the ZEUS measurement is consistent with the trend for $\langle k_T \rangle$ to rise with increasing W . This rise indicates that $\langle k_T \rangle$ should not be understood as purely intrinsic, due to parton confinement in the proton, but is probably the result of higher-order initial-state gluon radiation which increases with the phase space available.⁹

3 Deeply virtual Compton scattering

QCD-based calculations for DVCS have been performed by L. Frankfurt, A. Freund and M. Strikman (FFS)¹⁰ in terms of two gluon exchange with the proton as shown in Fig. 4. The calculations also include the purely electromagnetic Bethe-Heitler process, which dominates the total cross section for $e^+p \rightarrow e^+\gamma p$, together with the interference term.

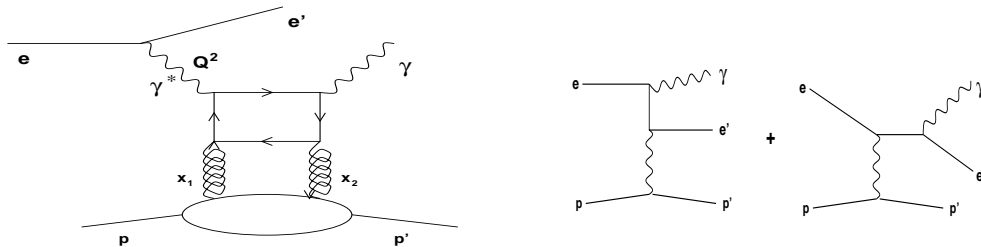


Figure 4: The quark box diagram on the left was used for the FFS calculation of the DVCS cross section at low x . The right-hand diagrams are for the Bethe-Heitler process.

Both ZEUS and H1 have developed Monte Carlo event generators based on these calculations. Studies by ZEUS have shown that it is possible to separate the DVCS signal from the Bethe-

Heitler background by selecting events in which there is a backward positron and a photon in the central or forward region (relative to the proton beam direction).

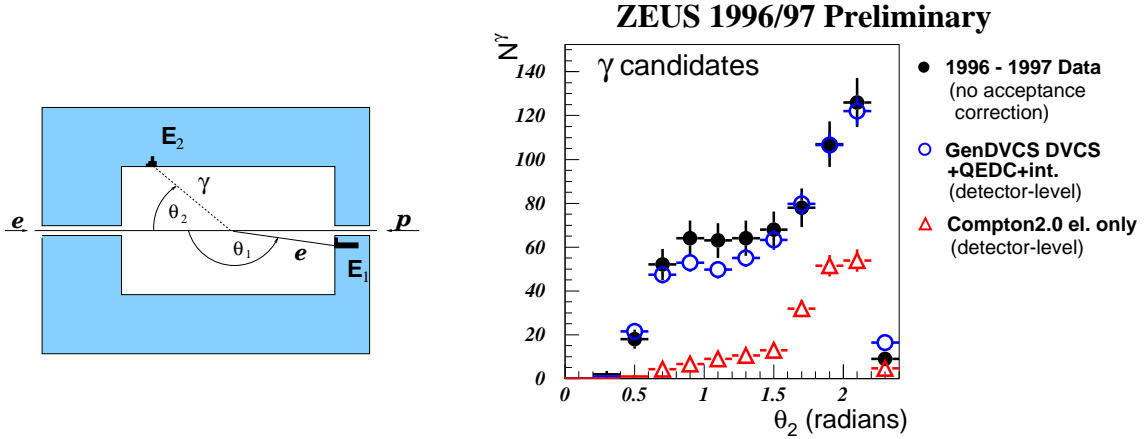


Figure 5: The schematic diagram on the left defines the variables used in the ZEUS selection of DVCS candidates. The right-hand plot shows the distribution of θ_2 compared to the Monte Carlo predictions for the Bethe-Heitler (QEDC) process with and without DVCS.

The first observation of DVCS at HERA was made by ZEUS using the selection cuts:

$$\begin{aligned} \theta_1 &> 2.8 \text{ rad} & E_1 &> 10 \text{ GeV} \\ \theta_2 &< 2.4 \text{ rad} & E_2 &> 2 \text{ GeV} \\ |\theta_1 - \theta_2| &> 0.8 \text{ rad} & Q^2 &> 6 \text{ GeV}^2 \end{aligned}$$

where the variables are as shown in Fig. 5. The photon shower shapes were studied and found to be incompatible with π^0 and η^0 production. As may be seen from Fig.5, there is a significant excess of events over the pure Bethe-Heitler prediction but the data agree well with the prediction of the DVCS plus Bethe-Heitler Monte Carlo generator.

The analysis of data from the H1 detector, which has been described elsewhere,¹¹ was also based on the requirement for two electromagnetic clusters, one with an energy above 15 GeV in the backward calorimeter and a second in the central part of the LAr calorimeter with $p_T > 1 \text{ GeV}$, where p_T is the transverse momentum with respect to the proton beam. To remove background, events were rejected if there were other clusters above 0.5 GeV or if signals were seen in the forward detectors. Events were also rejected if more than one track was found, or if the reconstructed track did not point to one of the clusters. If no track was seen, the backward cluster was assumed to be the positron.

For DVCS candidates, the photon was required to be in the central part of the calorimeter and the positron in the backward part. Events with the positron in the central part and the photon in the backward were used as a control sample. This consisted almost entirely of Bethe-Heitler events, with a negligible DVCS contribution, owing to the large scattering angle of the positron. However, there was a small background from diffractive ρ production and from electron pairs.

Figure 6 shows a number of distributions for the DVCS candidates compared to the Monte Carlo calculations for Bethe-Heitler events only. The large excess of events above the prediction is clear evidence for DVCS. Note in particular that the distribution of the coplanarity (the difference in azimuthal angle of the two clusters) is much broader than for the Bethe-Heitler process. This is because the diffractive DVCS events have a much flatter t dependence than the purely electromagnetic Bethe-Heitler process and so have a poorer p_T balance between the positron and photon.

An important check was made by studying the same distributions as plotted in Fig.6 for events in the control sample, instead of DVCS candidates. In this case there was good agreement

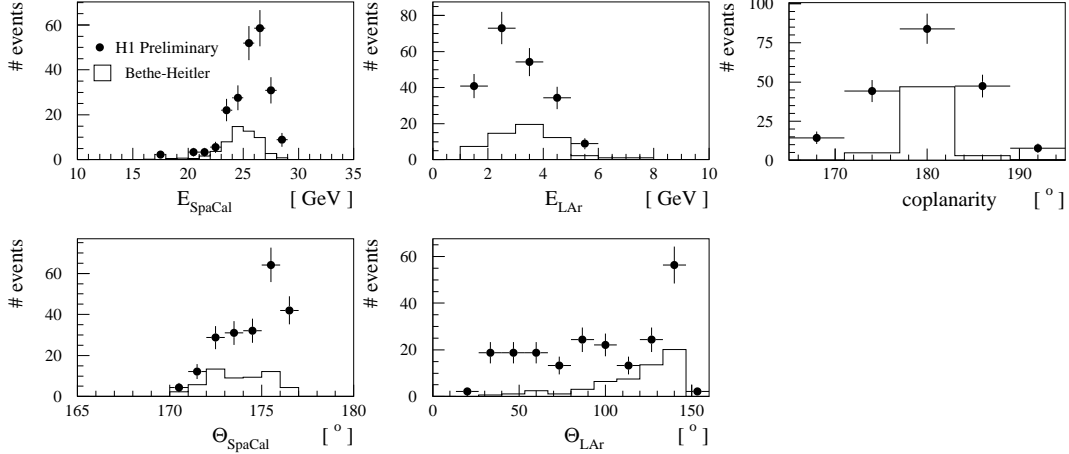


Figure 6: Uncorrected event distributions for the H1 DVCS candidates are compared to the Monte Carlo predictions for the Bethe-Heitler process only. The distributions are of the energy and polar angle of the two clusters, where LAr indicates the central calorimeter and SpaCal the backward one, and of the event coplanarity (see text).

between the data and the predictions of the Monte Carlo generator for the Bethe-Heitler process plus background, so indicating that the acceptance of the detector was well understood.

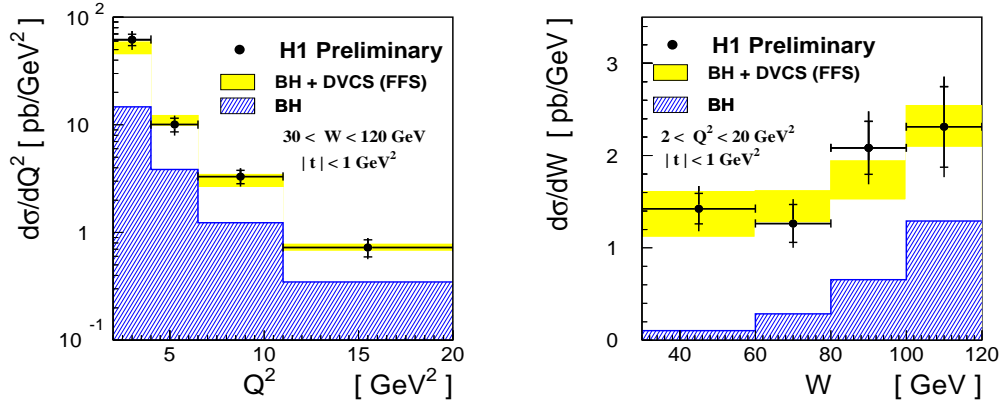


Figure 7: The cross sections for $e^+p \rightarrow e^+\gamma p$ measured by H1 as functions of Q^2 and W are compared to the FFS predictions. The predictions for the Bethe-Heitler process alone are also shown.

To calculate cross sections, the kinematics of the DVCS candidates was reconstructed by the double angle method and the Monte Carlo generator was used to correct for the detector acceptance. Figure 7 shows the differential cross sections as functions of Q^2 and W . The data are compared to the Monte Carlo predictions for the Bethe-Heitler process and for Bethe-Heitler plus DVCS (FFS).¹⁰ The range of the FFS prediction represents the uncertainty in the t dependence of the DVCS cross section. However, it is clear that the results are well described by the model.

4 Conclusions

Prompt photons provide a clean way to study QCD and photon structure. ZEUS has used such events to make a new determination of $\langle k_T \rangle$, the effective transverse parton momentum in the proton. This is consistent with the trend seen by other experiments for $\langle k_T \rangle$ to rise as W increases.

First signals for DVCS have been seen by both H1 and ZEUS. H1 has also measured cross sections which are in good agreement with QCD-based predictions. The interference between

DVCS and the Bethe-Heitler process is still to be investigated, but the better statistics expected after the HERA upgrade will be a great advantage.

Acknowledgments

I should like to thank the Moriond organisers for the invitation to attend a most stimulating conference. I am also grateful for many helpful discussions with my ZEUS and H1 colleagues.

References

1. ZEUS Collaboration, J. Breitweig *et al*, *Phys. Lett. B* **413**, 201 (1997).
2. A. Andresen *et al*, *Nucl. Instrum. Methods A* **309**, 101 (1999);
A. Bernstein *et al*, *Nucl. Instrum. Methods A* **338**, 23 (1993);
A. Caldwell *et al*, *Nucl. Instrum. Methods A* **321**, 356 (1992).
3. N. Harnew *et al*, *Nucl. Instrum. Methods A* **279**, 290 (1989);
B. Foster *et al*, *Nucl. Phys. B* (Proc. Suppl.) **32** (1993) 181; *Nucl. Instrum. Methods A* **338**, 254 (1994).
4. ZEUS Collaboration, J. Breitweig *et al*, *Phys. Lett. B* **472**, 175 (2000).
5. ZEUS Collaboration, J. Breitweig *et al*, *Eur. Phys. J. C* **6**, 43 (1999).
6. H.-U. Bengtsson and T. Sjöstrand, *Comp. Phys. Comm.* **46**, 43 (1987);
T. Sjöstrand, *Comp. Phys. Comm.* **82**, 74 (1994).
7. L. Apanasevich *et al*, *Phys. Rev. D* **59**, 074007 (1999);
L. Apanasevich *et al*, *Phys. Rev. D* **63**, 014009 (2001).
8. M. Begel, Ph. D. Thesis, University of Rochester, NY (1998).
9. E. Laenen, G. Sterman and W. Vogelsang, *Phys. Rev. Lett.* **84**, 4296 (2000).
10. L.L. Frankfurt, A. Freund and M. Strikman, *Phys. Rev. D* **58**, 114001 (1998); *Phys. Rev. D* **59**, 119901E (1999).
11. H1 Collaboration, I. Abt *et al*, *Nucl. Instrum. Methods A* **386**, 310 and 348 (1997).